Dynamical evolution of the Uranian satellite system

I. From the 5/3 Ariel–Umbriel mean motion resonance to the present

Sérgio R. A. Gomes[a,*], Alexandre C. M. Correia[a,b]

[a] *CFisUC, Departamento de Física, Universidade de Coimbra, 3004-516 Coimbra, Portugal*
[b] *IMCCE, UMR8028 CNRS, Observatoire de Paris, PSL Université, 77 Av. Denfert-Rochereau, 75014 Paris, France*

ABSTRACT

Mutual gravitational interactions between the five major Uranian satellites raise small quasi-periodic fluctuations on their orbital elements. At the same time, tidal interactions between the satellites and the planet induce a slow outward drift of the orbits, while damping the eccentricities and the inclinations. In this paper, we revisit the current and near past evolution of this system using a $N-$body integrator, including spin evolution and tidal dissipation with the weak friction model. We update the secular eigenmodes of the system and show that it is unlikely that any of the main satellites were recently captured into a high obliquity Cassini state. We rather expect that the Uranian satellites are in a low obliquity Cassini state and compute their values. We also show that the current eccentricities of the satellites are not forced, and estimate the free eccentricities and inclinations. We constrain the quality factor of Uranus to be $Q_U = (8.6 \pm 2.9) \times 10^3$, and that of the satellites to be $Q_S \sim 500$. We find that the system most likely encountered the 5/3 mean motion resonance between Ariel and Umbriel in the past, at about (0.7 ± 0.2) Gyr ago. We additionally determine the eccentricities and inclinations of all satellites just after the resonance passage that comply with the current system. We finally show that, from the crossing of the 5/3 MMR to the present, the evolution of the system is mostly peaceful and dominated by tides raised on Uranus by the satellites.

1. Introduction

The orbits of the five largest moons of Uranus pose many queries. Their proximity with the host planet and the short orbital periods make them a very compact system (Table 1), similar to many exoplanetary systems such as Trappist-1 (Gillon et al., 2017), Kepler-11 (Lissauer et al., 2011), TOI-178 (Leleu et al., 2021) or TOI-1136 (Dai et al., 2023). This places the Uranian system as a perfect laboratory to study in detail the formation and evolution of many close-in compact systems.

Uranus spin-axis has an extreme 98° inclination relatively to its orbital plane. Such poses the satellite's orbital plane almost perpendicular to the planet's orbital plane. Even so, Laskar and Robutel (1993) showed that the tilt of Uranus is stable and should be considered primordial. Moreover, the regular satellites are immune to solar perturbation and to the migration effects of the giant planets in the early solar system (Deienno et al., 2011). Therefore, the long-term evolution of the satellite's orbits can be conducted as an isolated system.

Natural satellites are believed to be formed in a protoplanetary disk around the host planet (e.g. Peale, 1999), or to be "free bodies" that were captured by the host planet (e.g. Singer, 1968; Agnor and Hamilton, 2006; Jewitt and Haghighipour, 2007). Despite the origin of the Uranian satellite system is not yet completely understood and still under debate (see Rogoszinski and Hamilton, 2021, for a detailed revision), the main satellites were likely formed in a circumplanetary disk (eg. Pollack et al., 1991; Szulágyi et al., 2018; Ishizawa et al., 2019; Inderbitzi et al., 2020; Ida et al., 2020; Rufu and Canup, 2022). Indeed, data from Voyager 2 shows that the distribution of mass between the satellites and Uranus and their chemical composition are consistent with these bodies having been condensed from a concentric disk, withstanding the idea that the regular moons of Uranus formed in an accretion disk around the planet (Prentice, 1986; Pollack et al., 1991). As a consequence, the initial eccentricities and inclinations of the main satellites should have been extremely small. Yet, the current inclination of Miranda of about 4.3° is considerably high when compared with the $\lesssim 0.1°$ inclinations of the remaining satellites (Tittemore and Wisdom, 1989, 1990; Malhotra and Dermott, 1990; Verheylewegen et al., 2013; Ćuk et al., 2020).

✉ sergio.ra.gomes@outlook.com (S.R.A. Gomes); acor@uc.pt (A.C.M. Correia)
ORCID(s): 0000-0001-9386-3996 (S.R.A. Gomes)

Table 1
Physical and mean orbital parameters of the five largest Uranian satellites. The masses and orbital parameters are from Jacobson (2014), the radius is from Thomas (1988), and the second order gravity field, J_2, and the tidal Love numbers are from Table 2 in Chen et al. (2014). The fluid potential Love number, k_f, and the inner structure coefficient, ζ, are obtained from Eq. (13) and (15), respectively.

	Uranus	Miranda	Ariel	Umbriel	Titania	Oberon
Mass ($\times 10^{-10}\,\mathrm{M_\odot}$)	$4.365\,628 \times 10^5$	0.323997	6.291561	6.412118	17.096471	15.468953
Radius (km)	25 559	235.8	578.9	584.7	788.4	761.2
J_2	3.5107×10^{-3}	6.10×10^{-3}	1.39×10^{-3}	6.13×10^{-4}	1.13×10^{-4}	1.48×10^{-5}
k_2	0.104	8.84×10^{-4}	1.02×10^{-3}	7.35×10^{-3}	1.99×10^{-2}	1.68×10^{-2}
k_f	0.356	0.907	0.862	1.016	0.899	0.790
ζ	0.225	0.327	0.320	0.342	0.326	0.310
Period (day)	0.718328	1.413480	2.520381	4.144176	8.705883	13.463254
$a\,(R_0)$		5.080715	7.470167	10.406589	17.069604	22.827536
$e\,(\times 10^{-3})$		1.35	1.22	3.94	1.23	1.40
$I\,(°)$		4.4072	0.0167	0.0796	0.1129	0.1478

The currently observed eccentricities of the Uranian satellites are also intriguing. Although small, they are still abnormally high when tidal dissipation is taken into account (e.g. Squyres et al., 1985). Tides are expected to damp the free eccentricity on a $10^7 - 10^8$ timescale, and the forced eccentricity oscillations owing to mutual perturbations between the satellites cannot explain the present values (Dermott and Nicholson, 1986; Laskar, 1986).

Since the formation of the Solar System, 4.5 Gyr ago, tidal friction is thought to induce a slow outward differential migration of the main five Uranian satellites (eg. Peale, 1988). The changes on the relative distances between the satellites most likely lead to the crossing of several commensurabilities in the past, where the most recent is believed to be 5/3 mean motion resonance (MMR) between Ariel and Umbriel. Previous studies focussed on the passage through the several low order MMRs possibly encountered by the major Uranian satellites during its orbital evolution (Tittemore and Wisdom, 1988; Ćuk et al., 2020; Gomes and Correia, 2023). They have shown that the passage through the 5/3 Ariel-Umbriel MMR, with or without long-term capture, most likely excited the eccentricities and inclinations of the three largest innermost satellites, shaping the current architecture of the system.

Ćuk et al. (2020) suggest that the 5/3 MMR between Ariel and Umbriel can also be responsible for the current high inclination of Miranda. However, the high inclination values around 1° also acquired by Ariel and Umbriel seem difficult to conciliate with the present observed system. An alternative scenario attributes Miranda's high inclination to passage through the 3/1 MMR between Miranda-Umbriel (Tittemore and Wisdom, 1989, 1990), thus making its passage somewhere in the past mandatory. A more plausible scenario is then that Miranda's inclination is excited during the Miranda and Umbriel 3/1 MMR crossing, and then Ariel and Umbriel skip the 5/3 MMR without being captured to prevent any damage on the inclinations.

Despite some studies on 5/3 MMR passage have been already conducted (Tittemore and Wisdom, 1988; Ćuk et al., 2020; Gomes and Correia, 2023), the orbital evolution of the main satellites just after this commensurability remain uncertain. Far from a resonance, tidal interactions between the satellites and Uranus are expected to dominate the evolution of the system. Thus, since the last MMR, the eccentricities and inclinations of the satellites should tend towards a state of equilibrium between the mutual perturbations within the satellites and tidal friction.

In this paper, we revisit the current and near past tidal evolution of the main five Uranian moons. We aim to understand the current architecture of the system and how the major satellites of Uranus settled into the present state. We start by access the present orbital status of the major Uranian satellites, in Sect. 2. Then, by adopting the weak friction tidal model, in Sect. 3, we study their impact in shaping the present system and derive constraints on the dissipation rates. Finally, in Sect.4 we attempt to reconstruct the tidal orbital evolution of the satellites from just after the passage through 5/3 MMR up to the present days. We discuss our results in Sect. 5. In a companion paper (Gomes and Correia, 2024), hereafter Paper II, we provide an exhaustive view on how the system evaded capture in the 5/3 MMR, allowing it to evolve into the present configuration.

Table 2
Position and velocity vectors at August, 1st, 1985, on the Earth equatorial frame of the five main satellites of Uranus (Jacobson, 2014).

Satellite	Position (km) (X, Y, Z)	Velocity (km.s^{-1}) $(\dot{X}, \dot{Y}, \dot{Z})$
Miranda	−127430.9607930668	−0.422514450329333
	23792.64617013941	−1.271890082631948
	−3464.554580724168	6.552338419694388
Ariel	−185785.2177189803	−0.384730129923274
	42477.81018746200	−1.393752472818678
	−2109.273462727150	5.325004225204424
Umbriel	−176566.9475784755	−3.350588413391897
	89016.12833946147	−0.153568184837806
	−3.350588413391897	3.273855499527411
Titania	−221240.1941919138	−3.049048602775958
	145452.9878060127	0.138409610142017
	−346697.1461249496	1.991437563896877
Oberon	−155108.4287158760	−2.962407899779837
	181606.6634411168	0.385864135361727
	−532879.3651011410	0.993694238058708

2. The present system

2.1. Orbital architecture

Jacobson (2014) provides the best precise estimation to date of the Uranian satellites. The masses, m, and the radius, R, of the planet and the satellites are given in Table 1. The position and velocity vectors of the satellite's orbits, expressed on the Earth's equatorial frame are given in Table 2.

Departing from the position vector, $\mathbf{R} = (X, Y, Z)$, and the velocity vector, $\dot{\mathbf{R}} = (\dot{X}, \dot{Y}, \dot{Z})$, we compute the corresponding osculating elliptical elements, that is, the semi-major axis, a, the eccentricity, e, the inclination, I, the mean longitude, λ, the longitude of the pericentre, ϖ, and the longitude of the ascending node, Ω, given in the Earth equatorial frame (e.g. Murray and Dermott, 1999). However, it is more convenient to express the orbital elements in the Uranian equatorial reference frame. We start from the Uranus' pole orientation declination and right ascension angles at August, 1st, 1985, respectively

$$\delta = 15.172593631449473° \, ,$$
$$RA = 77.31003302401596° \, ,$$
$$(1)$$

obtained from the Appendix B of Jacobson (2014). Then, by solving (e.g. Smart, 1965)

$$\cos \epsilon = \sin \delta \quad \text{and} \quad \cos \psi = -\frac{\cos \delta \sin(RA)}{\sin \epsilon} \, ,$$
$$(2)$$

we compute the angle between the spin axis and the vector normal to the orbital plane, i.e., the obliquity (ϵ), and the longitude of the Uranus' equator (ψ) in the Earth equatorial frame, respectively

$$\epsilon = 74.82740636855053° \, ,$$
$$\psi = 167.31003302401598° \, .$$
$$(3)$$

Finally, using spherical trigonometry to relate the Earth and Uranus equatorial frames (e.g. Smart, 1965), we obtain the osculating elliptical elements of the five major Uranian satellites expressed in the Uranus equatorial frame:

$$\cos I = \cos \epsilon \cos I' + \sin \epsilon \sin I' \cos (\Omega' - \psi) \, ,$$
$$(4)$$

$$\cos(\omega' - \omega) = \frac{\cos \epsilon - \cos I' \cos I}{\sin I' \sin I} \, ,$$
$$(5)$$

Table 3

Osculating elliptical orbital elements of the five main Uranian satellites on the Uranus' equatorial frame at August, 1st, 1985.

Satellite	$a\,(\times 10^{-3})$ (au)	$e\,(\times 10^{-3})$	$I\,(°)$
Miranda	0.867 829 806 096 133 50	1.514 384 267 990 232 1	4.409 022 644 189 928 3
Ariel	1.275 948 662 323 624 6	1.805 443 506 830 879 5	0.016 291 682 978 667 430
Umbriel	1.777 460 690 547 404 9	4.191 314 031 279 796 3	0.063 682 350 178 256 561
Titania	2.915 953 942 255 327 8	2.691 429 331 439 770 1	0.121 328 358 382 614 83
Oberon	3.899 495 282 248 682 5	1.021 848 548 198 646 7	0.158 417 224 439 574 40

	$\lambda\,(°)$	$\varpi\,(°)$	$\Omega\,(°)$
Miranda	358.880 308 531 500 816 1	316.937 899 650 424 299 1	32.632 119 491 654 876
Ariel	359.225 048 310 293 573 2	326.006 912 382 803 648 1	262.704 359 532 296 85
Umbriel	316.296 810 560 891 003 7	302.708 185 623 147 471 7	247.494 695 744 495 12
Titania	304.303 406 743 820 914 9	213.653 062 268 936 082 5	353.260 064 668 545 00
Oberon	289.110 959 574 207 015 5	110.661 368 547 315 277 1	51.710 122 333 743 321

$$\cos \Omega = \cos \Omega' \cos(\omega' - \omega) \\ \quad - \sin(\Omega' - \psi)\sin(\omega' - \omega)\cos I' ,$$

(6)

where the primed quantities are expressed in the Earth equatorial frame, the non-primed quantities are expressed in the Uranian equatorial frame, and $\omega = \varpi - \Omega$. The final results are given in Table 3.

2.2. Numerical code

In order to run the simulations on the Uranian satellite's system, we use the $N-$body numerical code SPINS (Correia, 2018), that takes into account satellite-satellite interactions, spin dynamics, rotational flattening, and tidal dissipation following to the weak friction model. The numerical results in this section can also be obtained using the open-source code TIDYMESS (Boekholt and Correia, 2023), with the option tidal_model = 2, which corresponds to the weak friction tidal model. Our numerical code is also equivalent to the numerical integrator SIMPL that was used by Ćuk et al. (2020).

2.3. Secular modes

As the Uranian satellites orbit the central planet, mutual gravitational interactions lead to quasi-periodic oscillations of the eccentricities and inclinations over broad periods of time, known as secular variations. Through semi-analytical simplified models, it is possible to estimate the frequencies of the eigenmodes associated to the eccentricity and inclination of each satellite, known as the secular modes (e.g. Dermott and Nicholson, 1986). These frequencies were estimated by Laskar (1986); Laskar and Jacobson (1987) using the analytical model GUST (General Uranian satellite theory). Later, Malhotra et al. (1989) revisited the results obtained with GUST, incorporating the effects of near first order mean motion resonances (Carpino et al., 1987; Milani et al., 1987). Since then, the estimations of the satellite masses were updated, as well as the orbital parameters (Jacobson, 2014), and so a recalculation of these frequencies is required.

Departing from the orbital solution from Table 3 and the physical properties from Table 1, we integrated the system composed by Uranus, Miranda, Ariel, Umbriel, Titania, and Oberon over 100 kyr, disregarding the tidal perturbations. Through the software TRIP (Gastineau and Laskar, 2011), we performed a frequency analysis of the orbits (Laskar, 1990, 1993) to determine the fundamental frequencies of the eccentricities (g_k) and inclinations (s_k) of the five major Uranian satellites. The results are shown in Table 4, alongside the results obtained by Laskar and Jacobson (1987) and Malhotra et al. (1989). The subscripts are given in ascending order of the semi-major axes of the satellites. We observe there is a good agreement between all frequency values in Table 4. We thus conclude that the orbital secular modes are neither very sensitive to the improvements of the physical parameters performed by Jacobson (2014) nor to the inclusion of the spins of all bodies in the system. For completeness, we also determine the amplitudes of the linear Lagrange-Laplace solution of $z = e\,e^{i\varpi}$ (Table 5) and $\eta = \sin(I/2)\,e^{i\Omega}$ (Table 6) for the five main satellites of Uranus, also obtained through frequency analysis.

Table 4

Secular modes of Miranda (g_1, s_1), Ariel (g_2, s_2), Umbriel (g_3, s_3), Titania (g_4, s_4), and Oberon (g_5, s_5), obtained through frequency analysis of the orbital evolution of the SPINS $N-$body code over 100 kyr (Sect. 2.3).

	GUST (deg/yr)	LONGSTOP (deg/yr)	SPINS (deg/yr)		GUST (deg/yr)	LONGSTOP (deg/yr)	SPINS (deg/yr)
g_1	20.082	20.117	20.0417	s_1	−20.309	−20.340	−20.2408
g_2	6.217	6.186	6.2271	s_2	−6.287	−6.239	−6.2363
g_3	2.865	2.848	2.8506	s_3	−2.836	−2.790	−2.7674
g_4	2.079	2.086	2.1652	s_4	−1.843	−1.839	−1.8309
g_5	0.386	0.410	0.4063	s_5	−0.259	−0.269	−0.2677

Table 5

Secular modes and amplitudes of the linear Lagrange-Laplace solution of $z = e\,\mathrm{e}^{\mathrm{i}\varpi}$ for the five main satellites of Uranus, obtained through frequency analysis of the orbital evolution of the numerical code over 100 kyr (Sect. 2.3).

			Miranda	Ariel	Umbriel	Titania	Oberon
freq.	(deg/yr)	ϕ_k (deg)	$A_k\,(\times 10^{-6})$	$A_k\,(\times 10^{-6})$	$A_k\,(\times 10^{-6})$	$A_k\,(\times 10^{-6})$	$A_k\,(\times 10^{-6})$
g_1	20.042	313.126	1299.535	2.966			
g_2	6.227	341.119	59.866	1131.602	211.089	56.805	17.024
g_3	2.851	314.931	59.659	812.716	3628.894	397.368	158.321
g_4	2.165	237.733	8.364	101.800	443.203	906.305	788.069
g_5	0.406	193.770	6.277	59.575	238.199	1260.953	1424.890

Table 6

Secular modes and amplitudes of the linear Lagrange-Laplace solution of $\eta = \sin(I/2)\mathrm{e}^{\mathrm{i}\Omega}$ for the five main satellites of Uranus, obtained through frequency analysis of the orbital evolution of the numerical code over 100 kyr (Sect. 2.3).

			Miranda	Ariel	Umbriel	Titania	Oberon
freq.	(deg/yr)	ϕ_k (deg)	$A_k\,(\times 10^{-6})$	$A_k\,(\times 10^{-6})$	$A_k\,(\times 10^{-6})$	$A_k\,(\times 10^{-6})$	$A_k\,(\times 10^{-6})$
s_1	−20.241	212.624	38 463.617	113.341	10.661	1.385	0.424
s_2	−6.236	21.667	7.403	113.440	23.628	0.341	0.002
s_3	−2.767	214.343	13.653	145.813	587.441	70.654	16.465
s_4	−1.831	284.152	8.891	82.185	306.054	655.985	541.981
s_5	−0.268	29.600	3.026	72.212	252.155	949.090	1143.359

2.4. Cassini states

Tidal effects are expected to push the obliquity of the satellites, ϵ, towards zero (e.g. Hut, 1980; Correia, 2009), unless an additional perturbation maintains a non-zero obliquity, known as Cassini state (e.g. Colombo, 1966; Ward, 1975; Correia, 2015). These states correspond to stable equilibria of the Hamiltonian and become the end point of tidal dissipation. More precisely, by decomposing the orbital solution for the inclination in the secular modes (Table 6),

$$\eta = \sin(I/2)\,\mathrm{e}^{\mathrm{i}\Omega} = \sum_k A_k \mathrm{e}^{\mathrm{i}(s_k t + \phi_k)}\,, \tag{7}$$

we can write for each satellite (e.g. Laskar and Robutel, 1993; Correia and Laskar, 2003; Levrard et al., 2007),

$$\dot{\epsilon} = \sum_k 2 s_k A_k \cos(\psi - s_k t + \phi_k) - T_\epsilon \sin \epsilon \,, \tag{8}$$

$$\dot{\psi} = -\alpha \cos \epsilon + \cot \epsilon \sum_k 2 s_k A_k \sin(\psi - s_k t + \phi_k)\,, \tag{9}$$

where α is the precession constant, s_k are the secular orbital nodal precession frequencies (Table 4), A_k and ϕ_k are the respective amplitude and phase of the orbital forcing (Table 6), and T_ϵ is the tidal torque (e.g. Correia and Valente, 2022). For small amplitude variations of the inclination, we have $|A_k| \ll 1$ (Table 6), and so the stable Cassini equilibria

Table 7
Comparison between the precession constant of a synchronous rotating satellite, α (Eq. (12)), and the numerical precession rate, $\dot\psi$ (Eq. (9)), obtained through frequency analysis with the SPINS $N-$body code (Sect. 2.2) for a near zero obliquity.

Satellite	α (deg/yr)	$|\dot\psi|$ (deg/yr)
Miranda	4164.7182	4078.5164
Ariel	542.6365	540.3787
Umbriel	136.4137	136.1541
Titania	12.5519	12.5696
Oberon	3.3546	3.1287

for the spin are given by (e.g. Ward and Hamilton, 2004; Levrard et al., 2007)

$$\tan \epsilon_1 \approx \frac{2A_k}{1 + \alpha/s_k} \, , \tag{10}$$

and

$$\cos \epsilon_2 \approx -\frac{s_k}{\alpha} \, . \tag{11}$$

For a given satellite in a near circular orbit, we have (e.g. Goldstein, 1950; Correia and Rodríguez, 2013)

$$\alpha \approx \frac{3}{2} \frac{n^2}{\omega} \frac{C - A}{C} = \frac{3}{2} \frac{n^2}{\omega} \left(J_2 + 2C_{22} \right) \zeta^{-1} \, , \tag{12}$$

where n is the orbital mean motion, ω is the rotational angular velocity, C and A are the maximal and minimal moments of inertia, respectively, J_2 and C_{22} are second order gravity field coefficients, and ζ is an inner structure coefficient. For a synchronous satellite ($\omega = n$), the gravity field coefficients and ζ can be related to the fluid potential Love number, k_f, as (e.g. Correia and Rodríguez, 2013)

$$J_2 = k_f \frac{5}{6} \left(\frac{m_0}{m} \right) \left(\frac{R}{a} \right)^3 \, , \tag{13}$$

$$C_{22} = \frac{k_f}{4} \left(\frac{m_0}{m} \right) \left(\frac{R}{a} \right)^3 = \frac{3}{10} J_2 \, , \tag{14}$$

and (e.g. Jeffreys, 1976)

$$\zeta = \frac{C}{mR^2} = \frac{2}{3} \left(1 - \frac{2}{5} \sqrt{\frac{4 - k_f}{1 + k_f}} \right) , \tag{15}$$

where m_0 is the mass of Uranus, and m and R are the mass and the radius of the satellite, respectively. From the J_2 values in Table 1, estimated by Chen et al. (2014), we can obtain k_f and then ζ for all satellites. Adopting the present semi-major axes of the satellites (Table 1), with Eq. (12) we finally estimate the precession constant (see Table 7).

Using the same method performed to estimate the secular modes (Sect. 2.3), the precession rate (Eq. (9)) can also be obtained using a frequency analysis. From the results of the integration of the Uranian system obtained in Sect. 2.3, we used TRIP to analyse the precession frequency of the satellites when the obliquity is nearly zero. This comparison is important, because the precession rate is also influenced by the perturbations of the remaining satellites in the system (Eq. (9)). The numerical results are also shown in Table 7. We observe that there is a good agreement between the two determinations, meaning that the precession of the satellites is indeed dominated by the gravitational torque of Uranus (Eq. (12)).

During the passage through the 5/3 MMR between Ariel and Umbriel, Ćuk et al. (2020) observed that all five moons had their inclinations excited. The effect on the inclination is particularly significant in Miranda because it has

Table 8
Equilibrium obliquities for Cassini state 1 (Eq. (10)) for each individual value of s_k and A_k from Table 6.

Satellite	Cassini state 1 (deg)				
	s_1	s_2	s_3	s_4	s_5
Miranda	2.2×10^{-2}	1.3×10^{-6}	1.1×10^{-6}	4.6×10^{-7}	2.3×10^{-8}
Ariel	5.1×10^{-4}	1.5×10^{-4}	8.6×10^{-5}	3.2×10^{-5}	4.1×10^{-6}
Umbriel	2.1×10^{-4}	1.3×10^{-4}	1.4×10^{-3}	4.8×10^{-4}	5.7×10^{-5}
Titania	4.2×10^{-4}	3.9×10^{-5}	2.3×10^{-3}	1.3×10^{-2}	2.4×10^{-3}
Oberon	5.7×10^{-5}	2.2×10^{-5}	1.4×10^{-2}	8.8×10^{-2}	1.2×10^{-2}

Table 9
Equilibrium obliquities for Cassini state 2 (Eq. (11)) for each individual value of s_k from Table 6.

Satellite	Cassini state 2 (deg)				
	s_1	s_2	s_3	s_4	s_5
Miranda	89.9	89.9	90.0	90.0	90.0
Ariel	87.9	89.3	89.7	89.8	90.0
Umbriel	81.5	87.4	88.8	89.2	89.9
Titania	-	60.2	77.3	81.6	88.8
Oberon	-	-	27.7	54.1	85.1

the smallest mass, which could explain its current high value. However, after leaving the resonance, the remaining four moons are all left with inclination values higher than the current ones. Ćuk et al. (2020) then propose that the inclination of Umbriel can be lowered if its node is involved in a secular spin-orbit resonance with the spin of Oberon, that is, if $\alpha_{\text{oberon}} \approx s_3$, which corresponds to Cassini state 2.

In Tables 8 and 9, we compute the equilibrium obliquities for all satellites and secular modes in Cassini state 1 (Eq. (10)) and Cassini state 2 (Eq. (11)), respectively. We observe that most resonant states (state 2) can only occur for obliquities higher than 60°. These high obliquities are unlikely and difficult to explain for tidally evolved close-in bodies such as the satellites of Uranus (e.g. Levrard et al., 2007). Moreover, in the scenario evoked by Ćuk et al. (2020), the initial obliquity must be close to zero and then grow to the high value as the inclination is damped owing to angular momentum exchanges (see also Correia et al., 2016). As a result, it is only possible to trigger this mechanism when $\alpha \sim s_k$.

The only case where this scenario seems possible is for Oberon, whose spin axis can resonate with s_3 and develop an obliquity of about 28° (Table 9), which is exactly the case reported by Ćuk et al. (2020). However, the non-zero obliquity would generate an excess of tidal energy dissipated within Oberon that would leave recent geological traces on its surface. Unfortunately, data from Voyager 2 have shown that, among the five regular moons, Oberon presents one of the most cratered and ancient surfaces (Smith et al., 1986; Plescia, 1987; Avramchuk et al., 2007). In addition, we would also need that other satellites simultaneously enter in resonance with s_2, s_4, and s_5, in order to damp the inclinations of Ariel, Titania and Oberon, respectively. Therefore, the scenario proposed by Ćuk et al. (2020) does not seem a suitable explanation to decrease the inclinations of the satellites after the passage through the 5/3 MMR between Ariel and Umbriel. We rather expect that the obliquities of the Uranian satellites present low obliquities corresponding to Cassini state 1 (Table 8).

3. Orbital evolution

Tidal effects arise from differential and inelastic deformations of an extended body owing to the gravitational effect of a perturber. The resulting dissipation of tidal energy modifies the spin and the orbit of the extended body. The final outcome corresponds to circular orbits, zero obliquity, and synchronous rotation (e.g. Hut, 1980). For a planet-satellite system, tides raised by the planet on the satellite are much stronger than tides raised by the satellite on the planet. Therefore, the satellite is expected to reach synchronous rotation on a short timescale, while the planetary spin continues to evolve slowly (e.g. Correia, 2009).

The dissipation of the mechanical energy of tides inside the extended body can be characterised by a time delay, τ, between the maximal deformation and the initial perturbation. As in many previous studies, we adopt here the weak

friction model (eg. Singer, 1968; Alexander, 1973; Mignard, 1979), which assumes a constant and small-time delay (Sect. 2.2). For a better understanding of the orbital evolution of the satellites, we show here the equations of motion for zero obliquity ($\epsilon = 0$), small eccentricity, and small inclination for this tidal model (e.g. Correia et al., 2011; Correia and Valente, 2022):

$$\frac{\dot{a}_k}{a_k} \approx \mathcal{K}_{k0} \left(\left(2 + 27 e_k^2 - I_k^2 \right) \frac{\omega_0}{n_k} - \left(2 + 46 e_k^2 \right) \right) + \mathcal{K}_{0k} \left(\left(2 + 27 e_k^2 - I_k^2 \right) \frac{\omega_k}{n_k} - \left(2 + 46 e_k^2 \right) \right) , \tag{16}$$

$$\frac{\dot{e}_k}{e_k} \approx \mathcal{K}_{k0} \left(\frac{11}{2} \frac{\omega_0}{n_k} - 9 \right) + \mathcal{K}_{0k} \left(\frac{11}{2} \frac{\omega_k}{n_k} - 9 \right) , \tag{17}$$

$$\frac{\dot{I}_k}{I_k} \approx -\mathcal{K}_{k0} \frac{\omega_0}{n_k} - \mathcal{K}_{0k} \left(\frac{\omega_k}{n_k} - 1 \right) , \tag{18}$$

with

$$\mathcal{K}_{k0} = k_{2,0} \frac{3 \mathcal{G} m_k^2 R_0^5}{\beta_k a_k^8} \tau_0 , \quad \text{and} \quad \mathcal{K}_{0k} = k_{2,k} \frac{3 \mathcal{G} m_0^2 R_k^5}{\beta_k a_k^8} \tau_k , \tag{19}$$

where $\mathcal{G}$ is the gravitational constant,

$$\beta_k = \frac{m_0 m_k}{m_0 + m_k} , \tag{20}$$

$k_{2,k}$ is the tidal second Love number, and τ_k is the time delay. The subscripts $_0$ and $_k$ pertain to Uranus and the satellite with index k, respectively.

Despite Miranda's relatively high inclination, the satellites present very small eccentricities and inclinations (Table 3) and they are expected to present synchronous rotation, that is, $\epsilon_k \approx e_k \approx I_k \approx 0$ and $\omega_k/n_k \approx 1$. Therefore, the orbital evolution can be further simplified as

$$\frac{\dot{a}_k}{a_k} \approx 2 \mathcal{K}_{k0} \left(\frac{\omega_0}{n_k} - 1 \right) , \tag{21}$$

$$\frac{\dot{e}_k}{e_k} \approx \mathcal{K}_{k0} \left(\frac{11}{2} \frac{\omega_0}{n_k} - 9 \right) - \frac{7}{2} \mathcal{K}_{0k} , \tag{22}$$

$$\frac{\dot{I}_k}{I_k} \approx -\mathcal{K}_{k0} \frac{\omega_0}{n_k} . \tag{23}$$

3.1. Outward migration

For the main satellites of Uranus, we always have $\omega_0/n_k \geq 2$ (Table 1). Thus, assuming synchronous rotation for the satellites, we conclude that the semi-major axes increase (Eq. (21)) and the orbits expand outwards. The evolution timescale depends on the time delay τ_0, which is related to the tidal dissipation inside Uranus.

A commonly used dimensionless quantity to measure the tidal dissipation is given by the quality factor (eg. Correia and Valente, 2022),

$$Q_0 \approx \frac{1}{2 \omega_0 \tau_0} \quad \text{and} \quad Q_k \approx \frac{1}{n_k \tau_k} . \tag{24}$$

Tittemore and Wisdom (1990) constrained the interval of Q_0 to be between $11\,000 - 39\,000$ by studying the likelihood of resonance crossing in the Uranian system. On one hand, they noticed that the 2/1 MMR between Ariel and Umbriel
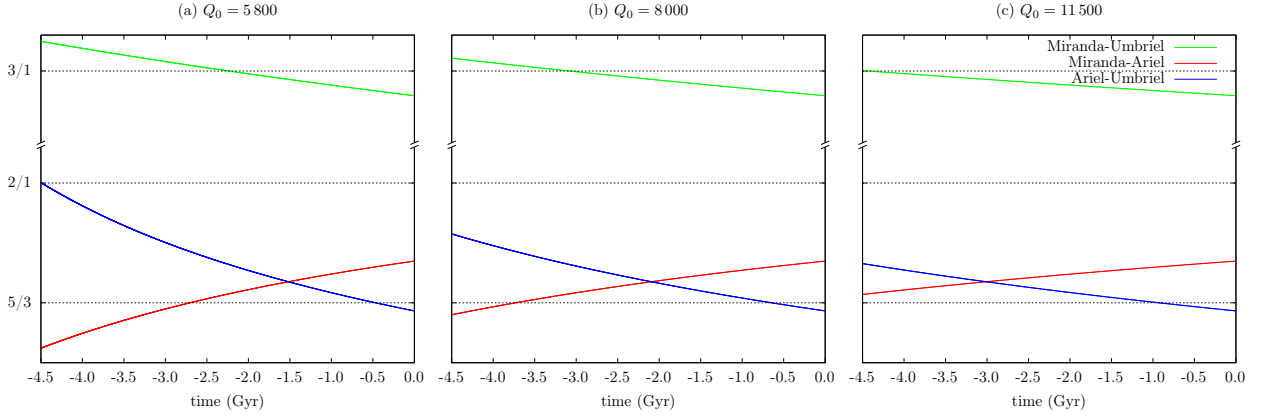
Figure 1: Backwards tidal evolution of the semi-major axes of Miranda, Ariel, and Umbriel using Eq. (21) with $Q_0 = 5\,800$ (a), $Q_0 = 8\,000$ (b), and $Q_0 = 11\,500$ (c). The green line gives the mean motion ratio between Miranda and Umbriel, the red line gives the same ratio for Miranda and Ariel, and the blue line is for Ariel and Umbriel. The dashed line gives the position of the nominal 3/1, 2/1, and 5/3 MMRs.

could not be crossed because the system is unable to evade it, and, on the other hand, the 3/1 MMR between Miranda and Umbriel should have been crossed such that we can explain the currently observed high inclination of Miranda (Tittemore and Wisdom, 1989).

Using the same approach, we recalculate the acceptable values for Q_0 using the weak friction tidal model and the updated parameters from Table 1. We start by estimating the current total angular momentum of the system projected on the direction of the spin axis of Uranus:

$$\Sigma = C_0 \omega_0 + \sum_{k=1}^{5} \left(C_k \omega_k \cos \epsilon_k + \beta_k \sqrt{\mu_k a_k (1 - e_k^2)} \cos I_k \right) , \tag{25}$$

with $\mu_k = \mathcal{G}(m_0 + m_k)$ and C_k is the moment of inertia of m_k (see Sect. 2.4). Adopting the current ω_0 and semi-major axes' values along with $\epsilon_k = e_k = I_k = 0$, and $\omega_k / n_k = 1$, we obtain

$$\Sigma = 9.446\,071 \times 10^{-10} \, \mathrm{M}_\odot \, \mathrm{au}^2 \, \mathrm{yr}^{-1} . \tag{26}$$

We then integrate Eq. (21) backwards for the five largest satellites of Uranus. The evolution of ω_0 is obtained using the conservation of Σ and considering that the satellites remain synchronous (Eq. (25)). In Fig. 1, we show the evolution of the mean motion ratios of Miranda, Ariel, and Umbriel. We observe that for $Q_0 < 5\,800$, the 2/1 MMR between Ariel and Umbriel is crossed (see Fig. 1 a), while for $Q_0 > 11\,500$, the 3/1 MMR between Miranda and Umbriel is not crossed (see Fig. 1 c). We thus constrain Q_0 within $5\,800 - 11\,500$, or conversely,

$$Q_0 = (8.6 \pm 2.9) \times 10^3 . \tag{27}$$

Similarly, from the Q_0 limits above, we can also estimate that the 5/3 MMR between Ariel and Umbriel was crossed within $460 - 920$ Myr ago, that is,

$$T_{5/3} = -(0.69 \pm 0.23) \, \mathrm{Gyr} . \tag{28}$$

As in Gomes and Correia (2023), we adopt $Q_0 = 8\,000$ as a suitable value for the tidal dissipation in Uranus for the remainder of this study and also in Paper II. From Eq. (24), we compute $\tau_0 \approx 0.62$ s. Actually, the exact dissipation rate depends on the product $k_{2,0}\,\tau_0$ (Eq. (21)). As in previous studies, in the present work we adopt $k_{2,0} = 0.104$ (Gavrilov and Zharkov, 1977), which translates into

$$\frac{k_{2,0}}{Q_0} = 1.3 \times 10^{-5} \quad \Leftrightarrow \quad k_{2,0}\,\tau_0 = 0.064 \, \mathrm{s} . \tag{29}$$

In Fig. 1 b, we also show the backwards tidal evolution of the mean motion ratios for $Q_0 = 8\,000$. From Eq. (21) we then estimate that the 5/3 MMR between Ariel and Umbriel was crossed about 640 Myr ago, with

$$a_1/R_0 = 7.39054\,, \quad a_2/R_0 = 10.38909\,. \tag{30}$$

3.2. Eccentricity damping

Contrarily to the semi-major axis, the evolution of the eccentricity (Eq. (22)) has two different contributions, one from tides raised in Uranus (term in $\mathcal{K}_{k0}$) and another from tides raised in the satellite (term in $\mathcal{K}_{0k}$).

In order to estimate $\mathcal{K}_{0k}$, we adopt the tidal Love numbers listed in Table 1 (for more details see Chen et al., 2014). For icy moons, we expect $Q_k \sim 10^2 - 10^3$ (eg. Murray and Dermott (1999)). We thus have $\mathcal{K}_{k0}/\mathcal{K}_{0k} \ll 1$, and so the eccentricity evolution (Eq. (22)) is controlled by tides raised on the satellites,

$$\frac{\dot{e}_k}{e_k} \approx -\frac{7}{2}\mathcal{K}_{0k}\,. \tag{31}$$

We conclude that tides damp the eccentricity in a timescale

$$\tau_{e,k} \approx \frac{2}{7\mathcal{K}_{0k}}\,. \tag{32}$$

Previous studies show that Ariel and Umbriel exit the 5/3 MMR with average eccentricities in the order of $e_k \sim 10^{-2}$ (Tittemore and Wisdom, 1988; Ćuk et al., 2020), a result that is also confirmed by our numerical simulations in Paper II. The current mean eccentricities of Ariel and Umbriel are $e_2 \sim e_3 \sim 10^{-3}$ (Table 10). Since the 5/3 MMR is expected to have been crossed about 640 Myr ago (Sect. 3.1), from Eq. (31) we estimate that $Q_2 \approx 500$ is the best suited value in order to damp the eccentricity of Ariel by an order of magnitude.

For the remainder of this study and also in Paper II, we adopt $Q_k = 500$ for all satellites. We then also obtain (Table 1)

$$\begin{aligned}
\frac{k_{2,1}}{Q_1} &= 1.77 \times 10^{-6} \quad \Leftrightarrow \quad k_{2,1}\,\tau_1 = 0.034 \text{ s}\,, \\
\frac{k_{2,2}}{Q_2} &= 2.04 \times 10^{-5} \quad \Leftrightarrow \quad k_{2,2}\,\tau_2 = 0.707 \text{ s}\,, \\
\frac{k_{2,3}}{Q_3} &= 1.47 \times 10^{-5} \quad \Leftrightarrow \quad k_{2,3}\,\tau_3 = 0.837 \text{ s}\,, \\
\frac{k_{2,4}}{Q_4} &= 3.98 \times 10^{-5} \quad \Leftrightarrow \quad k_{2,4}\,\tau_4 = 4.764 \text{ s}\,, \\
\frac{k_{2,5}}{Q_5} &= 3.36 \times 10^{-5} \quad \Leftrightarrow \quad k_{2,5}\,\tau_5 = 6.219 \text{ s}\,,
\end{aligned} \tag{33}$$

which yields (Eq. (32))

$$\begin{aligned}
\tau_{e,1} &= 1.25 \text{ Gyr}\,, \\
\tau_{e,2} &= 0.26 \text{ Gyr}\,, \\
\tau_{e,3} &= 3.50 \text{ Gyr}\,, \\
\tau_{e,4} &= 18.7 \text{ Gyr}\,, \\
\tau_{e,5} &= 155 \text{ Gyr}\,.
\end{aligned} \tag{34}$$

We conclude that tides are able to modify the eccentricities of Miranda, Ariel, and Umbriel over the age of the Solar System, but not those of Titania and Oberon.

3.3. Inclination damping

As for the eccentricity, tides always damp the inclination of the satellites (Eq. (18)). However, the evolution of the inclination is essentially governed by tides raised on Uranus (Eq. (23)), as it happens for the semi-major axes (Eq. (21)). The timescale to damp the inclinations is then

$$\tau_{I,k} \approx \frac{1}{\mathcal{K}_{k0}}\,, \tag{35}$$

Table 10

Free orbital elements of the regular Uranus satellites, with and without the influence of the Sun.

Satellite	e_{min}	e_{mean}	e_{max}	I_{min} (°)	I_{mean} (°)	I_{max} (°)
Without the Sun						
Miranda	8.62×10^{-4}	1.31×10^{-3}	1.76×10^{-3}	4.404	4.409	4.414
Ariel	5.77×10^{-5}	1.29×10^{-3}	2.25×10^{-3}	7.92×10^{-4}	2.51×10^{-2}	5.90×10^{-2}
Umbriel	2.20×10^{-3}	3.67×10^{-3}	5.06×10^{-3}	2.41×10^{-3}	7.55×10^{-2}	1.36×10^{-1}
Titania	2.43×10^{-5}	1.64×10^{-3}	3.48×10^{-3}	2.48×10^{-2}	1.22×10^{-1}	1.93×10^{-1}
Oberon	3.64×10^{-5}	1.75×10^{-3}	3.46×10^{-3}	6.62×10^{-2}	1.39×10^{-1}	1.96×10^{-1}
With the Sun						
Miranda	8.44×10^{-4}	1.31×10^{-3}	1.76×10^{-3}	4.373	4.409	4.445
Ariel	5.27×10^{-5}	1.29×10^{-3}	2.31×10^{-3}	8.70×10^{-5}	2.72×10^{-2}	8.50×10^{-2}
Umbriel	2.21×10^{-3}	3.53×10^{-3}	5.18×10^{-3}	5.09×10^{-4}	7.35×10^{-2}	1.67×10^{-1}
Titania	1.95×10^{-5}	1.64×10^{-3}	3.50×10^{-3}	1.58×10^{-2}	1.32×10^{-1}	2.59×10^{-1}
Oberon	2.96×10^{-5}	1.82×10^{-3}	3.44×10^{-3}	4.55×10^{-2}	1.72×10^{-1}	2.74×10^{-1}

which yields about

$$
\begin{aligned}
\tau_{I,1} &= 290\,\text{Gyr}\,, \\
\tau_{I,2} &= 170\,\text{Gyr}\,, \\
\tau_{I,3} &= 1\,500\,\text{Gyr}\,, \\
\tau_{I,4} &= 14\,300\,\text{Gyr}\,, \\
\tau_{I,5} &= 105\,000\,\text{Gyr}\,.
\end{aligned}
\tag{36}
$$

We conclude that tides are thus very inefficient to damp the inclination of all the satellites. Indeed, since $\tau_{I,k} \gg \tau_{e,k}$, contrarily to the eccentricity, the present inclinations were likely almost unchanged since the system encountered the 5/3 MMR, and can be seen as fossilised values.

3.4. Free and forced orbital elements

Without tidal friction, the secular oscillations of the eccentricity and inclination are quasi-periodic and constrained within a given range, known as free oscillations (e.g. Laskar, 1986). As tidal friction damps the eccentricities and the inclinations of the satellites (Sects. 3.2 and 3.3), the system evolves into an equilibrium state uniquely dominated by its secular modes (Table 4), known as forced oscillations (e.g. Murray and Dermott, 1999).

To estimate the average free orbital elements, we disabled tidal effects and integrate the current configuration of the Uranian system (Table 3) over 50 000 years. Furthermore, in addition to the five regular satellites, we performed one integration which also included the Sun and another without it. The results are presented in Table 10. We note that there are no significant differences with and without the gravitational effect from the Sun, despite the high obliquity of Uranus. Such happens because Uranus is one of the outermost planets of the Solar System, and perturbations from the Sun are three orders of magnitude smaller than those from the satellites. These results confirm that the Uranian system can thus be analysed as an isolated system within our Solar System.

To evaluate the forced orbital elements, we integrated the system departing from the current configuration, as for the free orbital elements (Table 3). However, we now consider the tidal dissipation within the satellites, that is, $\tau_k \neq 0$. We do not include the tidal dissipation within Uranus ($\tau_0 = 0$), such that the semi-major axes do not increase (Eq. (21)). This approximation is justified because only the eccentricities are expected to evolve during the age of the Solar System and their evolution is dominated by tides raised by Uranus on the satellites (Eq. (31)).

To ensure that the free eccentricities are completely damped, we need to integrate the system over a very long time span, which is computationally expensive. One solution to decrease the computation time is to enhance the tidal strength by artificially increasing τ_k and then rescale the evolution time by the same factor. This approximation is valid as long as the tidal evolution is adiabatic and also possible because the tidal evolution is proportional to τ_k (Eq. (19)).

We start by comparing the results from different tidal multiplication factors, ×10, ×100, and ×1000. In Fig. 2, we superimposed the eccentricity of Miranda resulting from an integration over 20 Myr, 2 Myr and 0.2 Myr, where, for each simulation, we rescaled the time axis by the respective multiplication factor. We observe that the general evolution
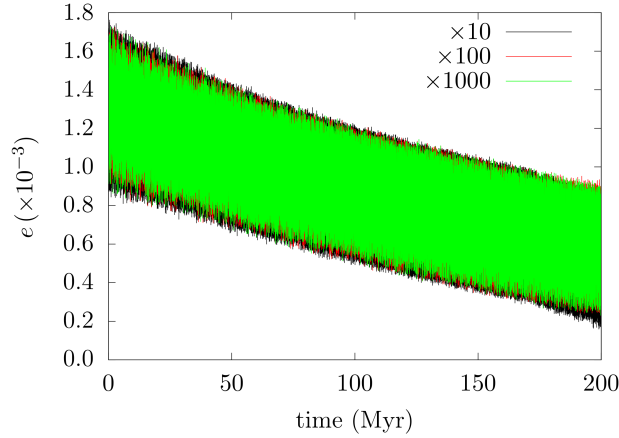
Figure 2: Evolution of the eccentricity of Miranda with three distinct time lags τ_1': $\tau_1'/\tau_1 = 10$ (black), $\tau_1'/\tau_1 = 100$ (red), and $\tau_1'/\tau_1 = 1000$ (green).

Table 11
Forced eccentricities for the major Uranian satellites. The values were numerically obtained by integrating the current system for 10 Gyr and disregarding tidal effects from Uranus (Fig. 3).

Satellite	e_{mean}	τ_e
Miranda	2.1×10^{-4}	1.3 Gyr
Ariel	1.5×10^{-4}	0.7 Gyr
Umbriel	6.0×10^{-4}	2.9 Gyr
Titania	$< 1.3 \times 10^{-3}$	> 10 Gyr
Oberon	$< 1.3 \times 10^{-3}$	> 10 Gyr

of the orbital elements is not sensitive to the enhancement of the tidal strength. Therefore, we conclude that we can speed up at least ×1000 the computation time without compromising the results. We note that it is not feasible to determine the forced inclinations through this method because we assume $\tau_0 = 0$ (Sect. 3.3). Anyway, the damping time-scale of the inclinations is several orders of magnitude larger than the age of the Solar System (Eq. (36)), and so we only need to focus our analysis on the eccentricities.

With a multiplication factor of ×1000, we integrated the system over 10 Gyr departing from the current orbital configuration (Table 3). The evolution of the eccentricity for all satellites is shown in Fig. 3. In Table 11, we list the numerical estimation of the damping timescale for all satellites. We observe that the eccentricities of Miranda, Ariel, and Umbriel are damped in less than 3 Gyr, which is in good agreement with the theoretical estimations obtained with a single satellite (Eq. (34)). For Titania and Oberon, the decrease in eccentricity over 10 Gyr is small when compared with the other innermost moons, and so we cannot determine neither the damping timescale nor the forced eccentricities, we can only put upper limits. In Table 11, we provide the mean values of the eccentricity obtained during the last Gyr of evolution, which correspond to the forced eccentricity oscillations. We observe that for Miranda, Ariel, and Umbriel, the forced eccentricity has an amplitude that is about one order of magnitude smaller than the currently observed values (Table 10). As a consequence, we conclude that some mechanism must have excited the current eccentricities of the three innermost Uranian satellites in a not so distant past (less than 1 Gyr).

4. Past evolution

The backwards tidal evolution of the semi-major axes obtained in Sect. 3.1 disregards the mutual perturbations of the satellites. As long as no mean motion resonances are encountered, we expect that the evolution of the complete system does not differ much from the asymptotical evolution provided by Eq. (21). The same reasoning is also valid for the evolution of the eccentricities (Eq. (22)) and inclinations (Eq. (23)).
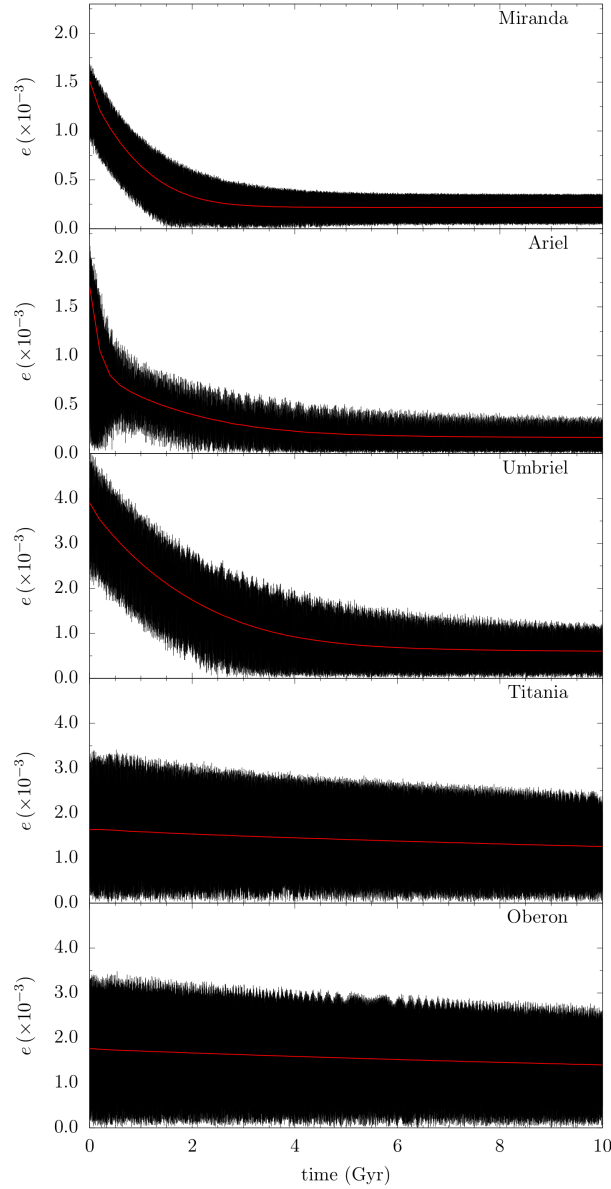
Figure 3: Forced eccentricities of the major Uranian satellites over 10 Gyr of tidal orbital evolution. The red line gives the average value of the eccentricity.

The closest past lower order mean motion resonance is the 5/3 MMR between Ariel and Umbriel (Fig. 1). The crossing of this resonance shifts the semi-major axes from their asymptotic values and greatly excites the eccentricities (see Paper II). As a consequence, we cannot extend beyond that point the backwards analysis from Sect. 3.1. However, three-body resonances may also impact the orbital evolution of the system in a near past and set the semi-major axis on a different track (e.g. Greenberg, 1975; Ćuk et al., 2020). Indeed, at present the orbit of Miranda is perturbed by a three-body Laplace resonance with Ariel and Umbriel, with the argument $\lambda_1 - 3\lambda_2 + 2\lambda_3$ (Greenberg, 1975; Jacobson, 2014). Therefore, in order to remount to the past evolution of the system, we cannot rely on the asymptotic evolution (Sect. 3.1) and need to take into account the complete N−body model described in Sect. 2.2.

The resonance crossing is a stochastic and irreversible process, and so we cannot just reverse the time and integrate the system into the past. We need to place the system where we think it was and then integrate it forwards aiming to reproduce the present observations. The crossing of the 5/3 MMR is studied in detail in Paper II. Here, we follow the

evolution from just after the passage through the 5/3 MMR until the present day. In order to guess the initial conditions, we adopt the asymptotic equations for the semi-major axes (Eq. 21) and eccentricities (Eq. (22)), leading to

$$
\begin{aligned}
a_1/R_0 &= 5.0584 , & e_1 &= 2.7 \times 10^{-3} , \\
a_2/R_0 &= 7.3959 , & e_2 &= 8.0 \times 10^{-3} , \\
a_3/R_0 &= 10.3900 , & e_3 &= 4.5 \times 10^{-3} , \\
a_4/R_0 &= 17.0645 , & e_4 &= 2.0 \times 10^{-3} , \\
a_5/R_0 &= 22.8234 , & e_5 &= 2.0 \times 10^{-3} .
\end{aligned}
\tag{37}
$$

For the inclinations, we adopt the present values (Table 1), as they are not expected to vary much (Sect. 3.3), except for Miranda's inclination, which was slightly increased to 4.41° to match the current inclination at the end of the simulation. The initial rotations of the satellites are synchronous with the orbital mean motion ($\omega_k/n_k = 1$), and the initial obliquities were set to zero ($\epsilon_k = 0°$). We then performed 100 simulations, where, for each run, we randomly choose the remaining orbital parameters ($\lambda_k, \varpi_k, \Omega_h$) between 0° and 360°. For the dissipation, we adopt the values given by expressions (29) and (33).

In Fig. 4, we display one example of the evolution of the semi-major axes, eccentricities, inclinations and obliquities, resulting from the integration of these initial conditions. As expected, we confirm that no two-body MMR was crossed. More importantly, we observe that the system is not captured in any three-body mean motion resonance either, and the migration rates are in excellent agreement with the asymptotic predictions (Eq. (21)). The final eccentricities and inclinations are also in perfect agreement with the currently observed values (Table 1). Moreover, we also observe that, starting from $\epsilon_k = 0°$, the obliquities of all satellites quickly evolve into the low obliquity Cassini state 1 (see Table 8), corroborating that it is unlikely for the satellites to become involved in the resonant high obliquity Cassini state 2, as suggested by Ćuk et al. (2020).

Similar results were observed in all the 100 simulations that we performed. No unexpected event deviated the system from its course, and all the 100 simulations correctly reproduced the current system. Our simulations cannot rule out a different evolution scenario, but it should certainly have a low probability. Therefore, we conclude that, after the passage through the 5/3 MMR between Ariel and Umbriel, the evolution of the system is mostly peaceful and dominated by tides raised on Uranus by the satellites.

5. Summary and Discussion

In the short-term, the variations in the orbits of Uranus's largest satellites are governed by mutual perturbations. However, the past long-term evolution is driven by tidal effects between the planet and its satellites. In this work, we have studied the present dynamics and the recent tidal evolution of these moons, namely, Miranda, Ariel, Umbriel, Titania, and Oberon. For that purpose, we have used a $N-$body code that takes into account satellite-satellite interactions, spin dynamics, and tidal dissipation.

We begun our study by accessing the present orbital configuration of the system. Departing from more recent data given by Jacobson (2014), we recomputed the secular modes of the five main satellites using the frequency analysis method (as in Laskar, 1986; Laskar and Jacobson, 1987). With these updated values, we accessed the possibility of spin-orbit resonances within the major satellites of Uranus. Ćuk et al. (2020) suggested that the current high inclination of Miranda could be explained due to the crossing of the 5/3 MMR between Ariel and Umbriel. In this scenario, the inclinations of all secular modes are excited, but their amplitude could then be lowered through spin-orbit resonances. We show that the only possibility is for a resonance between the precession of the spin axis of Oberon and the s_3 secular mode. Therefore, it is not feasible to damp the amplitude of the remaining secular models through this mechanism, and a more suitable explanation for the high inclination of Miranda remains the crossing of the 3/1 MMR between Miranda and Umbriel (Tittemore and Wisdom, 1989, 1990).

Tittemore and Wisdom (1990) argue that the 2/1 MMR between Miranda and Ariel could not have been crossed in the past, because capture is certain and the system cannot evade it. On the other hand, the system has to cross the 3/1 MMR between Miranda and Umbriel to increase the inclination of Miranda. Using these constraints, we updated the quality factor of Uranus to be $5\,800 < Q_0 < 11\,500$, which extends beyond the previously established range outlined by Tittemore and Wisdom (1990). This is a consequence of the improvement in the determination of the physical parameters of the satellites, namely, in the radii and the masses (Jacobson, 2014). Another consequence is that the encounter with the 5/3 MMR between Ariel and Umbriel must have occurred about 460 to 920 Myr ago.

The crossing of the 5/3 MMR excites the eccentricities of all satellites, but we show that tides quickly erode those of Miranda, Ariel, and Umbriel. In order to comply with the currently observed eccentricity values, we estimate that the quality factor of the satellites must be $Q_S \sim 500$. The inclinations remain essentially unchanged and can therefore be used as a fossilised signature of the system that emerged after the 5/3 MMR.

By performing a large number of numerical simulations, we finally show that, from the passage through the 5/3 MMR to the present, the system is not captured in any three-body mean motion resonance. As a result, the orbital evolution of each satellite follows the tidal evolution derived from an unperturbed two-body problem. In the companion Paper II (Gomes and Correia, 2024), we provide an exhaustive study on the crossing of the 5/3 MMR that sticks with the analysis presented here.

Acknowledgements

References

Agnor, C.B., Hamilton, D.P., 2006. Neptune's capture of its moon Triton in a binary-planet gravitational encounter. Nature 441, 192–194. doi:10.1038/nature04792.

Alexander, M.E., 1973. The Weak Friction Approximation and Tidal Evolution in Close Binary Systems. Astrophysics and Space Science 23, 459–510. doi:10.1007/BF00645172.

Avramchuk, V.V., Rosenbush, V.K., Bul'Ba, T.P., 2007. Photometric study of the major satellites of Uranus. Solar System Research 41, 186–202. doi:10.1134/S0038094607030021.

Boekholt, T.C.N., Correia, A.C.M., 2023. A direct N-body integrator for modelling the chaotic, tidal dynamics of multibody extrasolar systems: TIDYMESS. Monthly Notices of the Royal Astronomical Society] 522, 2885–2900. doi:10.1093/mnras/stad1133, arXiv:2209.03955.

Carpino, M., Milani, A., Nobili, A.M., 1987. Long-term numerical integrations and synthetic theories for the motion of the outer planets. Astronomy and Astrophysics 181, 182–194.

Chen, E.M.A., Nimmo, F., Glatzmaier, G.A., 2014. Tidal heating in icy satellite oceans. Icarus 229, 11–30. doi:10.1016/j.icarus.2013.10.024.

Colombo, G., 1966. Cassini's second and third laws. The Astronomical Journal 71, 891–896.

Correia, A.C.M., 2009. Secular Evolution of a Satellite by Tidal Effect: Application to Triton. The Astrophysical Journal Letters 704, L1–L4. doi:10.1088/0004-637X/704/1/L1, arXiv:0909.4210.

Correia, A.C.M., 2015. Stellar and planetary Cassini states. Astronomy and Astrophysics 582, A69. doi:10.1051/0004-6361/201525939.

Correia, A.C.M., 2018. Chaotic dynamics in the (47171) Lempo triple system. Icarus 305, 250–261. doi:10.1016/j.icarus.2018.01.008, arXiv:1710.08401.

Correia, A.C.M., Boué, G., Laskar, J., 2016. Secular and tidal evolution of circumbinary systems. Celestial Mechanics and Dynamical Astronomy 126, 189–225. doi:10.1007/s10569-016-9709-9, arXiv:1608.03484.

Correia, A.C.M., Laskar, J., 2003. Long-term evolution of the spin of Venus II. Numerical simulations. Icarus 163, 24–45. doi:10.1016/S0019-1035(03)00043-5.

Correia, A.C.M., Laskar, J., Farago, F., Boué, G., 2011. Tidal evolution of hierarchical and inclined systems. Celestial Mechanics and Dynamical Astronomy 111, 105–130. doi:10.1007/s10569-011-9368-9, arXiv:1107.0736.

Correia, A.C.M., Rodríguez, A., 2013. On the Equilibrium Figure of Close-in Planets and Satellites. The Astrophysical Journal 767, 128. doi:10.1088/0004-637X/767/2/128, arXiv:1304.1425.

Correia, A.C.M., Valente, E.F.S., 2022. Tidal evolution for any rheological model using a vectorial approach expressed in Hansen coefficients. Celestial Mechanics and Dynamical Astronomy 134, 24. doi:10.1007/s10569-022-10079-3, arXiv:2306.03449.

Ćuk, M., El Moutamid, M., Tiscareno, M.S., 2020. Dynamical History of the Uranian System. Plan. Sci. J. 1, 22. doi:10.3847/PSJ/ab9748, arXiv:2005.12887.

Dai, F., Masuda, K., Beard, C., Robertson, P., Goldberg, M., Batygin, K., Bouma, L., Lissauer, J.J., Knudstrup, E., Albrecht, S., Howard, A.W., Knutson, H.A., Petigura, E.A., Weiss, L.M., Isaacson, H., Kristiansen, M.H., Osborn, H., Wang, S., Wang, X.Y., Behmard, A., Greklek-McKeon, M., Vissapragada, S., Batalha, N.M., Brinkman, C.L., Chontos, A., Crossfield, I., Dressing, C., Fetherolf, T., Fulton, B., Hill, M.L., Huber, D., Kane, S.R., Lubin, J., MacDougall, M., Mayo, A., Močnik, T., Akana Murphy, J.M., Rubenzahl, R.A., Scarsdale, N., Tyler, D., Zandt, J.V., Polanski, A.S., Schwengeler, H.M., Terentev, I.A., Benni, P., Bieryla, A., Ciardi, D., Falk, B., Furlan, E., Girardin, E., Guerra, P., Hesse, K.M., Howell, S.B., Lillo-Box, J., Matthews, E.C., Twicken, J.D., Villaseñor, J., Latham, D.W., Jenkins, J.M., Ricker, G.R., Seager, S., Vanderspek, R., Winn, J.N., 2023. TOI-1136 is a Young, Coplanar, Aligned Planetary System in a Pristine Resonant Chain. The Astronomical Journal 165, 33. doi:10.3847/1538-3881/aca327, arXiv:2210.09283.

Deienno, R., Yokoyama, T., Nogueira, E.C., Callegari, N., Santos, M.T., 2011. Effects of the planetary migration on some primordial satellites of the outer planets. I. Uranus' case. Astronomy and Astrophysics 536, A57. doi:10.1051/0004-6361/201014862.

Dermott, S.F., Nicholson, P.D., 1986. Masses of the satellites of Uranus. Nature 319, 115–120. doi:10.1038/319115a0.

Gastineau, M., Laskar, J., 2011. Trip: A computer algebra system dedicated to celestial mechanics and perturbation series. ACM Commun. Comput. Algebra 44, 194–197. URL: http://doi.acm.org/10.1145/1940475.1940518, doi:10.1145/1940475.1940518.

Gavrilov, S.V., Zharkov, V.N., 1977. Love Numbers of the Giant Planets. Icarus 32, 443–449. doi:10.1016/0019-1035(77)90015-X.

Gillon, M., Triaud, A.H.M.J., Demory, B.O., Jehin, E., Agol, E., Deck, K.M., Lederer, S.M., de Wit, J., Burdanov, A., Ingalls, J.G., Bolmont, E., Leconte, J., Raymond, S.N., Selsis, F., Turbet, M., Barkaoui, K., Burgasser, A., Burleigh, M.R., Carey, S.J., Chaushev, A., Copperwheat, C.M., Delrez, L., Fernandes, C.S., Holdsworth, D.L., Kotze, E.J., Van Grootel, V., Almleaky, Y., Benkhaldoun, Z., Magain, P., Queloz, D., 2017. Seven temperate terrestrial planets around the nearby ultracool dwarf star TRAPPIST-1. Nature 542, 456–460. doi:10.1038/nature21360, arXiv:1703.01424.

Goldstein, H., 1950. Classical mechanics.

Gomes, S.R.A., Correia, A.C.M., 2023. Effect of the inclination in the passage through the 5/3 mean motion resonance between Ariel and Umbriel. Astronomy and Astrophysics 674, A111. doi:10.1051/0004-6361/202346101, arXiv:2305.08794.

Gomes, S.R.A., Correia, A.C.M., 2024. Dynamical evolution of the Uranian satellite system II. Crossing of the 5/3 Ariel–Umbriel mean motion resonance. arXiv e-prints .

Greenberg, R., 1975. On the Laplace relation among the satellites of Uranus. Monthly Notices of the Royal Astronomical Society] 173, 121–129. doi:10.1093/mnras/173.1.121.

Hut, P., 1980. Stability of tidal equilibrium. Astronomy and Astrophysics 92, 167–170.

Ida, S., Ueta, S., Sasaki, T., Ishizawa, Y., 2020. Uranian satellite formation by evolution of a water vapour disk generated by a giant impact. Nature Astronomy 4, 880–885. doi:10.1038/s41550-020-1049-8, arXiv:2003.13582.

Inderbitzi, C., Szulágyi, J., Cilibrasi, M., Mayer, L., 2020. Formation of satellites in circumplanetary discs generated by disc instability. Monthly Notices of the Royal Astronomical Society] 499, 1023–1036. doi:10.1093/mnras/staa2796, arXiv:1912.11406.

Ishizawa, Y., Sasaki, T., Hosono, N., 2019. Can the Uranian Satellites Form from a Debris Disk Generated by a Giant Impact? The Astrophysical Journal 885, 132. doi:10.3847/1538-4357/ab48ef, arXiv:1909.13065.

Jacobson, R.A., 2014. The Orbits of the Uranian Satellites and Rings, the Gravity Field of the Uranian System, and the Orientation of the Pole of Uranus. The Astronomical Journal 148, 76. doi:10.1088/0004-6256/148/5/76.

Jeffreys, H., 1976. The earth. Its origin, history and physical constitution. Cambridge University Press.

Jewitt, D., Haghighipour, N., 2007. Irregular Satellites of the Planets: Products of Capture in the Early Solar System. Annual Review of Astronomy and Astrophysics 45, 261–295. doi:10.1146/annurev.astro.44.051905.092459, arXiv:astro-ph/0703059.

Laskar, J., 1986. A general theory for the Uranian satellites. Astronomy and Astrophysics 166, 349–358.

Laskar, J., 1990. The chaotic motion of the solar system - A numerical estimate of the size of the chaotic zones. Icarus 88, 266–291. doi:10.1016/0019-1035(90)90084-M.

Laskar, J., 1993. Frequency analysis for multi-dimensional systems. Global dynamics and diffusion. Physica D Nonlinear Phenomena 67, 257–281. doi:10.1016/0167-2789(93)90210-R.

Laskar, J., Jacobson, R.A., 1987. GUST86 - an analytical ephemeris of the Uranian satellites. Astronomy and Astrophysics 188, 212–224.

Laskar, J., Robutel, P., 1993. The chaotic obliquity of the planets. Nature 361, 608–612. doi:10.1038/361608a0.

Leleu, A., Alibert, Y., Hara, N.C., Hooton, M.J., Wilson, T.G., Robutel, P., Delisle, J.B., Laskar, J., Hoyer, S., Lovis, C., Bryant, E.M., Ducrot, E., Cabrera, J., Delrez, L., Acton, J.S., Adibekyan, V., Allart, R., Allende Prieto, C., Alonso, R., Alves, D., Anderson, D.R., Angerhausen, D., Anglada Escudé, G., Asquier, J., Barrado, D., Barros, S.C.C., Baumjohann, W., Bayliss, D., Beck, M., Beck, T., Bekkelien, A., Benz, W., Billot, N., Bonfanti, A., Bonfils, X., Bouchy, F., Bourrier, V., Boué, G., Brandeker, A., Broeg, C., Buder, M., Burdanov, A., Burleigh, M.R., Bárczy, T., Cameron, A.C., Chamberlain, S., Charnoz, S., Cooke, B.F., Corral Van Damme, C., Correia, A.C.M., Cristiani, S., Damasso, M., Davies, M.B., Deleuil, M., Demangeon, O.D.S., Demory, B.O., Di Marcantonio, P., Di Persio, G., Dumusque, X., Ehrenreich, D., Erikson, A., Figueira, P., Fortier, A., Fossati, L., Fridlund, M., Futyan, D., Gandolfi, D., García Muñoz, A., Garcia, L.J., Gill, S., Gillen, E., Gillon, M., Goad, M.R., González Hernández, J.I., Guedel, M., Günther, M.N., Haldemann, J., Henderson, B., Heng, K., Hogan, A.E., Isaak, K., Jehin, E., Jenkins, J.S., Jordán, A., Kiss, L., Kristiansen, M.H., Lam, K., Lavie, B., Lecavelier des Etangs, A., Lendl, M., Lillo-Box, J., Lo Curto, G., Magrin, D., Martins, C.J.A.P., Maxted, P.F.L., McCormac, J., Mehner, A., Micela, G., Molaro, P., Moyano, M., Murray, C.A., Nascimbeni, V., Nunes, N.J., Olofsson, G., Osborn, H.P., Oshagh, M., Ottensamer, R., Pagano, I., Pallé, E., Pedersen, P.P., Pepe, F.A., Persson, C.M., Peter, G., Piotto, G., Polenta, G., Pollacco, D., Poretti, E., Pozuelos, F.J., Queloz, D., Ragazzoni, R., Rando, N., Ratti, F., Rauer, H., Raynard, L., Rebolo, R., Reimers, C., Ribas, I., Santos, N.C., Scandariato, G., Schneider, J., Sebastian, D., Sestovic, M., Simon, A.E., Smith, A.M.S., Sousa, S.G., Sozzetti, A., Steller, M., Suárez Mascareño, A., Szabó, G.M., Ségransan, D., Thomas, N., Thompson, S., Tilbrook, R.H., Triaud, A., Turner, O., Udry, S., Van Grootel, V., Venus, H., Verrecchia, F., Vines, J.I., Walton, N.A., West, R.G., Wheatley, P.J., Wolter, D., Zapatero Osorio, M.R., 2021. Six transiting planets and a chain of Laplace resonances in TOI-178. Astronomy and Astrophysics 649, A26. doi:10.1051/0004-6361/202039767, arXiv:2101.09260.

Levrard, B., Correia, A.C.M., Chabrier, G., Baraffe, I., Selsis, F., Laskar, J., 2007. Tidal dissipation within hot Jupiters: a new appraisal. Astronomy and Astrophysics 462, L5–L8. doi:10.1051/0004-6361:20066487, arXiv:astro-ph/0612044.

Lissauer, J.J., Ragozzine, D., Fabrycky, D.C., Steffen, J.H., Ford, E.B., Jenkins, J.M., Shporer, A., Holman, M.J., Rowe, J.F., Quintana, E.V., Batalha, N.M., Borucki, W.J., Bryson, S.T., Caldwell, D.A., Carter, J.A., Ciardi, D., Dunham, E.W., Fortney, J.J., Gautier, Thomas N., I., Howell, S.B., Koch, D.G., Latham, D.W., Marcy, G.W., Morehead, R.C., Sasselov, D., 2011. Architecture and Dynamics of Kepler's Candidate Multiple Transiting Planet Systems. The Astrophysical Journal Supplement 197, 8. doi:10.1088/0067-0049/197/1/8, arXiv:1102.0543.

Malhotra, R., Dermott, S.F., 1990. The role of secondary resonances in the orbital history of Miranda. Icarus 85, 444–480. doi:10.1016/0019-1035(90)90126-T.

Malhotra, R., Fox, K., Murray, C.D., Nicholson, P.D., 1989. Secular perturbations of the Uranian satellites: theory and practice. Astronomy and Astrophysics 221, 348–358.

Mignard, F., 1979. The Evolution of the Lunar Orbit Revisited. I. Moon and Planets 20, 301–315. doi:10.1007/BF00907581.

Milani, A., Nobili, A.M., Carpino, M., 1987. Secular variations of the semimajor axes - Theory and experiments. Astronomy and Astrophysics 172, 265–279.

Murray, C.D., Dermott, S.F., 1999. Solar system dynamics. Cambridge University Press.

Peale, S.J., 1988. Speculative histories of the Uranian satellite system. Icarus 74, 153–171. doi:10.1016/0019-1035(88)90037-1.

Peale, S.J., 1999. Origin and Evolution of the Natural Satellites. Annual Review of Astronomy and Astrophysics 37, 533–602. doi:10.1146/annurev.astro.37.1.533.

Plescia, J.B., 1987. Cratering history of the Uranian satellites: Umbriel, Titania, and Oberon. Journal of Geophysical Research 92, 14918–14932. doi:10.1029/JA092iA13p14918.

Pollack, J.B., Lunine, J.I., Tittemore, W.C., 1991. Origin of the Uranian satellites., in: Bergstralh, J.T., Miner, E.D., Matthews, M.S. (Eds.), Uranus, pp. 469–512.

Prentice, A.J.R., 1986. Uranus after Voyager 2 and the origin of the solar system. Proceedings of the Astronomical Society of Australia 6, 394–402.

Rogoszinski, Z., Hamilton, D.P., 2021. Tilting Uranus: Collisions versus Spin-Orbit Resonance. Plan. Sci. J. 2, 78. doi:10.3847/PSJ/abec4e, arXiv:2004.14913.

Rufu, R., Canup, R.M., 2022. Coaccretion + Giant-impact Origin of the Uranus System: Tilting Impact. The Astrophysical Journal 928, 123. doi:10.3847/1538-4357/ac525a, arXiv:2204.00124.

Singer, S.F., 1968. The Origin of the Moon and Geophysical Consequences. Geophysical Journal International 15, 191–204. doi:10.1111/j.1365-246X.1968.tb05758.x.

Smart, W.M., 1965. Text-book on spherical astronomy. Cambridge University Press.

Smith, B.A., Soderblom, L.A., Beebe, R., Bliss, D., Boyce, J.M., Brahic, A., Briggs, G.A., Brown, R.H., Collins, S.A., Cook, A.F., Croft, S.K., Cuzzi, J.N., Danielson, G.E., Davies, M.E., Dowling, T.E., Godfrey, D., Hansen, C.J., Harris, C., Hunt, G.E., Ingersoll, A.P., Johnson, T.V., Krauss, R.J., Masursky, H., Morrison, D., Owen, T., Plescia, J.B., Pollack, J.B., Porco, C.C., Rages, K., Sagan, C., Shoemaker, E.M., Sromovsky, L.A., Stoker, C., Strom, R.G., Suomi, V.E., Synnott, S.P., Terrile, R.J., Thomas, P., Thompson, W.R., Veverka, J., 1986. Voyager 2 in the Uranian System: Imaging Science Results. Science 233, 43–64. doi:10.1126/science.233.4759.43.

Squyres, S.W., Reynolds, R.T., Lissauer, J.J., 1985. The enigma of the Uranian satellites' orbital eccentricities. Icarus 61, 218–223. doi:10.1016/0019-1035(85)90103-4.

Szulágyi, J., Cilibrasi, M., Mayer, L., 2018. In Situ Formation of Icy Moons of Uranus and Neptune. The Astrophysical Journal Letters 868, L13. doi:10.3847/2041-8213/aaeed6, arXiv:1811.06574.

Thomas, P.C., 1988. Radii, shapes, and topography of the satellites of Uranus from limb coordinates. Icarus 73, 427–441. doi:10.1016/0019-1035(88)90054-1.

Tittemore, W.C., Wisdom, J., 1988. Tidal evolution of the Uranian satellites I. Passage of Ariel and Umbriel through the 5:3 mean-motion commensurability. Icarus 74, 172–230. doi:10.1016/0019-1035(88)90038-3.

Tittemore, W.C., Wisdom, J., 1989. Tidal evolution of the Uranian satellites II. An explanation of the anomalously high orbital inclination of Miranda. Icarus 78, 63–89. doi:10.1016/0019-1035(89)90070-5.

Tittemore, W.C., Wisdom, J., 1990. Tidal evolution of the Uranian satellites III. Evolution through the Miranda-Umbriel 3:1, Miranda-Ariel 5:3, and Ariel-Umbriel 2:1 mean-motion commensurabilities. Icarus 85, 394–443. doi:10.1016/0019-1035(90)90125-S.

Verheylewegen, E., Noyelles, B., Lemaitre, A., 2013. A numerical exploration of Miranda's dynamical history. Monthly Notices of the Royal Astronomical Society] 435, 1776–1787. doi:10.1093/mnras/stt1415, arXiv:1302.4329.

Ward, W.R., 1975. Tidal friction and generalized Cassini's laws in the solar system. The Astronomical Journal 80, 64–70.

Ward, W.R., Hamilton, D.P., 2004. Tilting Saturn. I. Analytic Model. The Astronomical Journal 128, 2501–2509. doi:10.1086/424533.
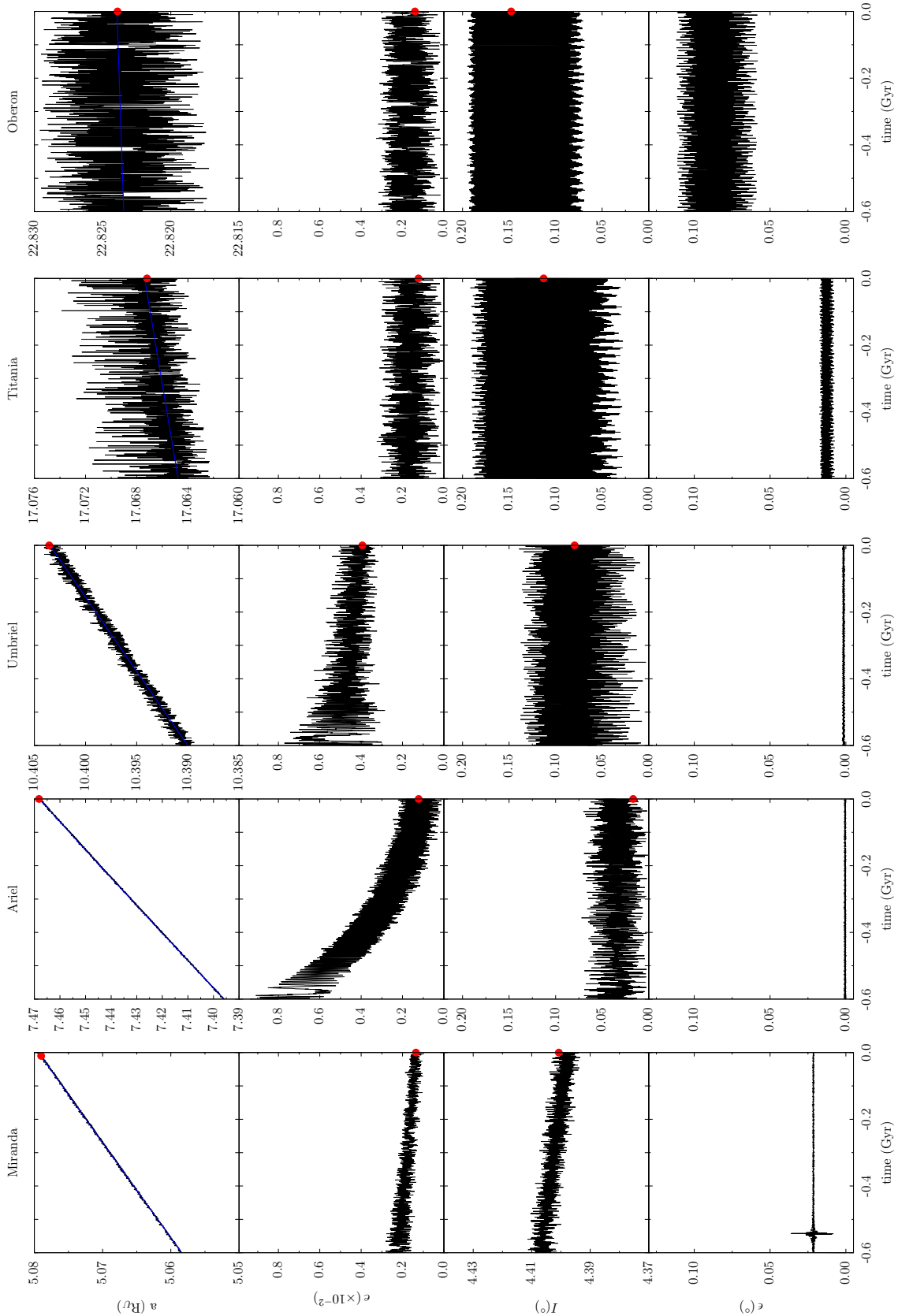
Figure 4: Orbital and spin evolution of the five main satellites of Uranus from 600 Myr ago to the present. The blue line is the asymptotic evolution of the semi-major axes, obtained by Eq. (21). From the top to the bottom, we show the semi-major axes, the eccentricities, the inclinations, and the obliquities. The current mean orbital parameters (Table 10) were superimposed as red circles.